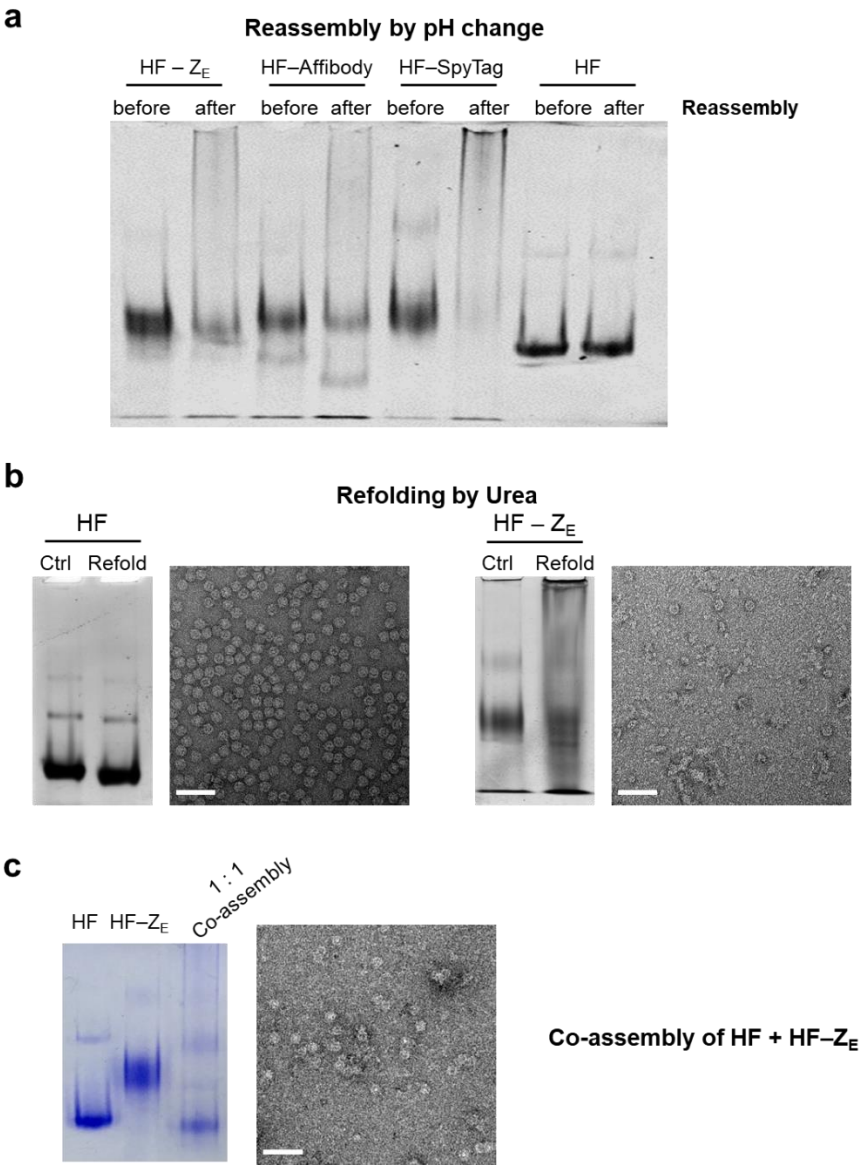

Figure S1. Reassembly and refolding of protein/peptide fused ferritins. (a) Native gel image of ferritin variants fused with leucine zipper, Z_E (HF-Z_E), small affibody (~6 kDa) (HF-affibody), SpyTag peptide (HF-SpyTag) as well as intact wild type ferritin (HF) before and after pH-dependent cage reassembly. (b) Native gel and TEM images of HF and HF-Z_E before and after urea-dependent cage refolding. (c) Native gel and TEM images of HF, HF-Z_E and HF+HF-Z_E mixture before and after pH-dependent cage reassembly (co-assembly for the HF+HF-Z_E mixture). All scale bars 50 nm.

Note: Although wild type ferritin (HF) is fully reassembled and refolded into the 24-meric cage structure, large portions of protein/peptide-fused ferritins are not properly reassembled and refolded (Figures S1a, S1b). More importantly, co-assembled structures between HF and HF-Z_E are highly heterogeneous, which also contains many defected cages.

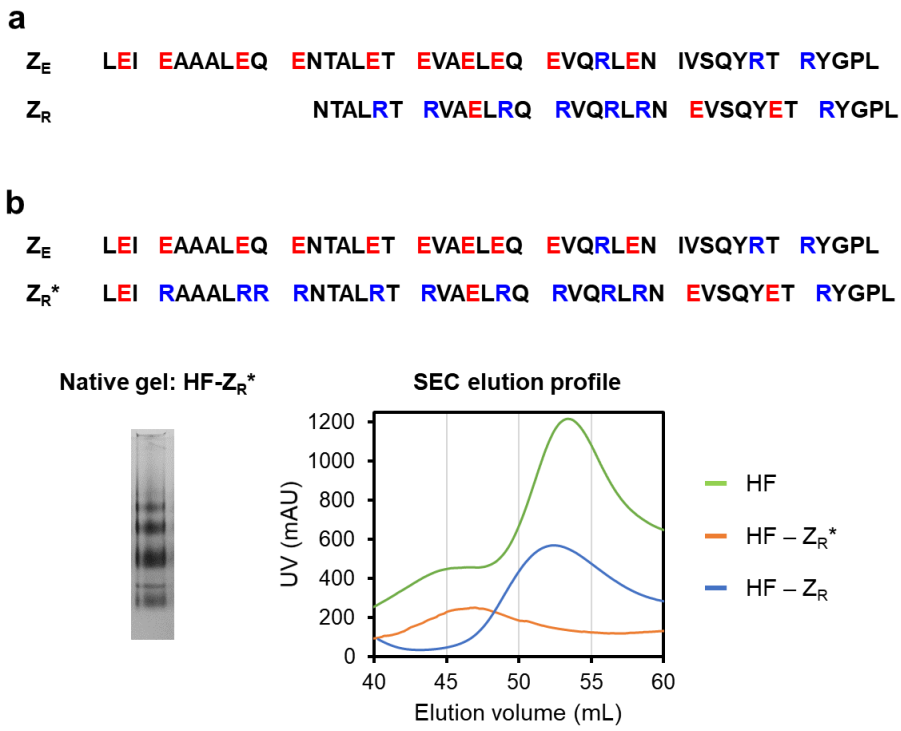

Figure S2. Leucine zippers for cage-to-cage assembly. (a) Z_E and Z_R sequences. Negative glutamic acid and positive arginine residues are indicated with red and blue, respectively. (b) Z_R truncation. The original full-length Z_R* sequence is listed. The native gel band pattern for HF-Z_R* and size exclusion chromatography (SEC) elution profiles of HF, HF-Z_R*, HF-Z_R are shown.

Note: The original full-length Z_R* has a homo-dimerization tendency with K_D ~10^{-7} M, and consequently, expressed HF-Z_R* are multimerized as shown in native gel and SEC data (Figure S2b). Here, we removed 11 amino acids from the N-terminus of Z_R* to prevent this homo-dimerization. The truncated Z_R was fused to HF, and the resulting HF-Z_R showed no multimerization but still strongly interacted with the Z_E peptide.

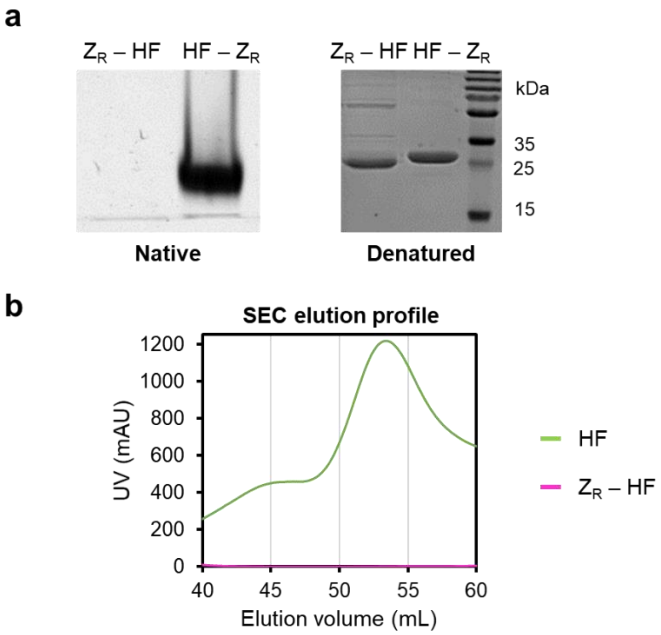

Figure S3. Z_R fused ferritin preparation. (a) Native and denatured gel images of N-terminal and C-terminal fused Z_R ferritins. (b) SEC profiles of wild type ferritin (HF, green) and Z_R-HF (magenta). The N-terminal fused Z_R-HF was not folded into the cage structure.

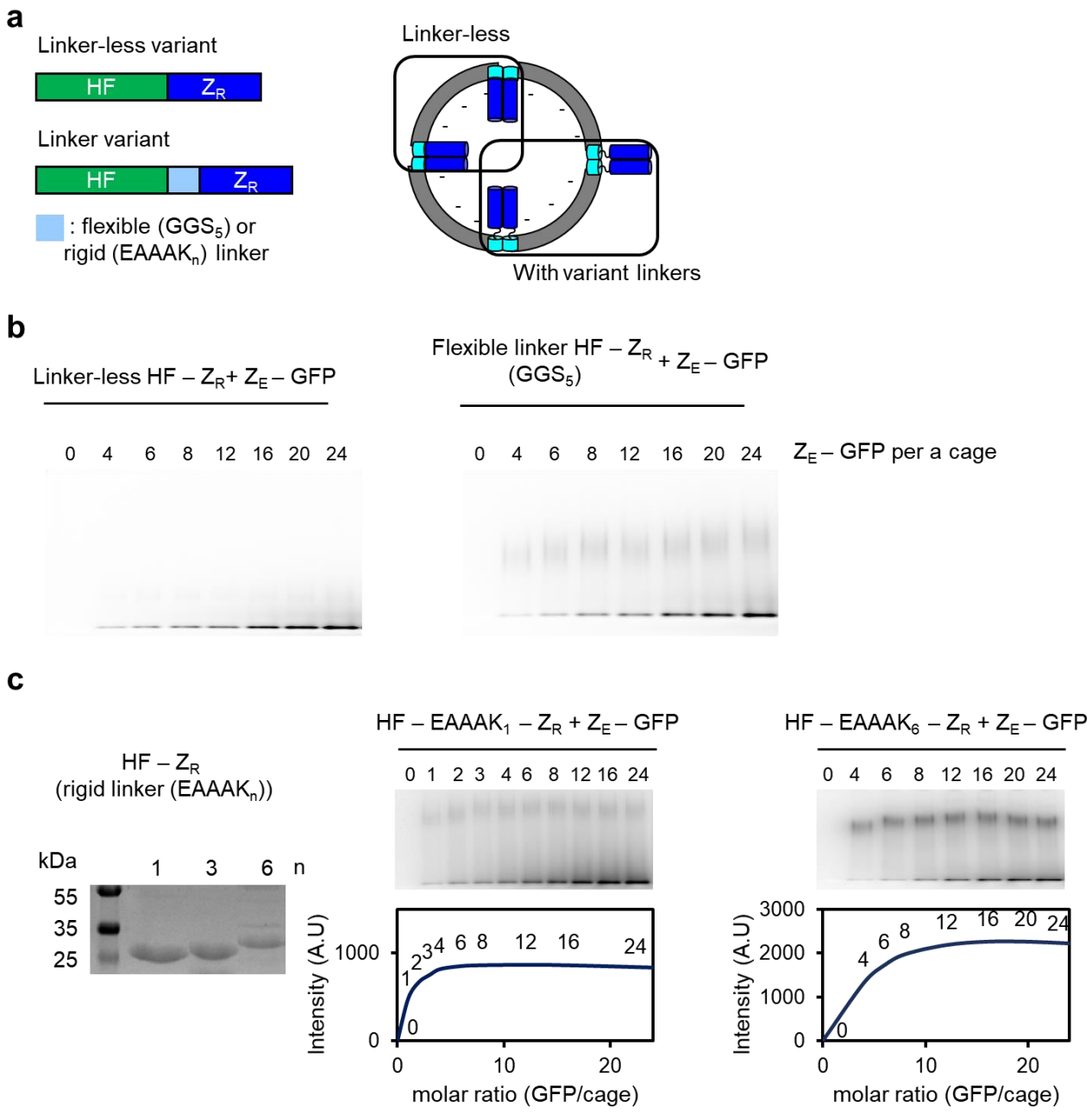

Figure S4. HF-Z_R flopping by different linkers. (a) Schematics of HF-Z_R linker variants. (b) Native gel images of Z_E-GFP binding to linker-less HF-Z_R and long flexible linker HF-Z_R with varying GFP/cage ratios. (c) Native gel images of Z_E-GFP binding to short rigid linker ($EAAAK_1$) HF-Z_R and long rigid linker ($EAAAK_6$) HF-Z_R with varying GFP/cage ratios. A SDS-PAGE gel image of purified HF-Z_R rigid linker variants was shown in the left.

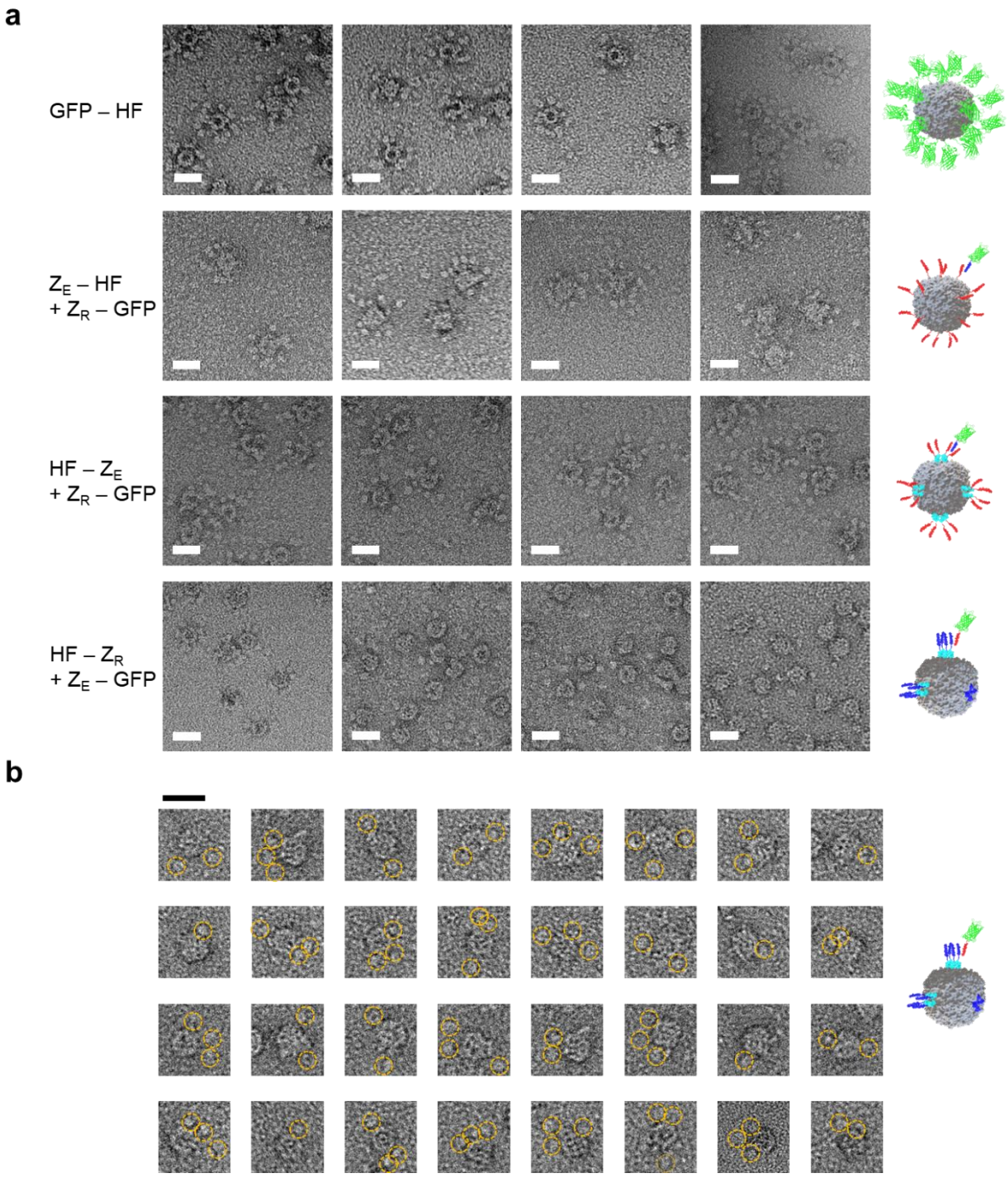

Figure S5. TEM images of GFP-bound ferritin variants. (a) Additional TEM images and schematic structures of GFP-fused HF (GFP-HF) and zipper-fused ferritin variants bound with their complementary zipper-fused GFPs. (b) Enlarged TEM images of HF-Z_R+Z_E-GFP complexes. Stained GFPs around HF-Z_R are indicated with dotted yellow circles. Scale bars 20 nm.

Note: Mixtures of zipper-fused ferritin variants and their complementary zipper-fused GFPs were applied for SEC to remove unbound GFPs before TEM analysis.

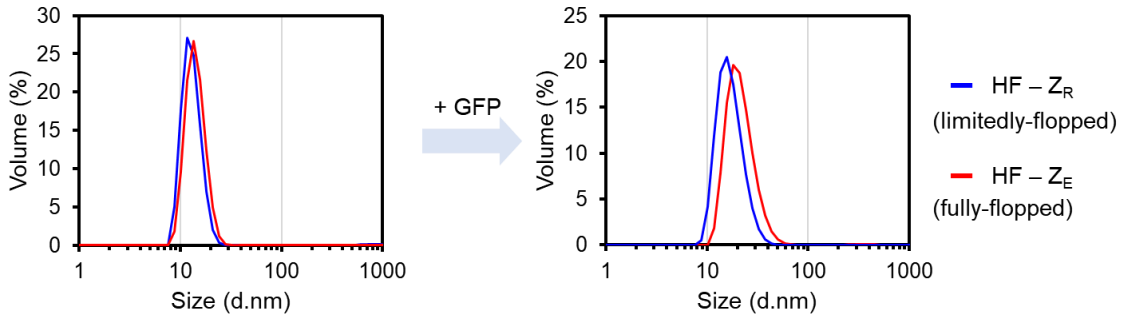

Figure S6. Dynamic Light Scattering (DLS) data of HF-Z_E and HF-Z_R before (left) and after (right) GFP binding.

Note: Mixtures of zipper-fused ferritin variants and their complementary zipper-fused GFPs were applied for SEC to remove unbound GFPs before DLS analysis.

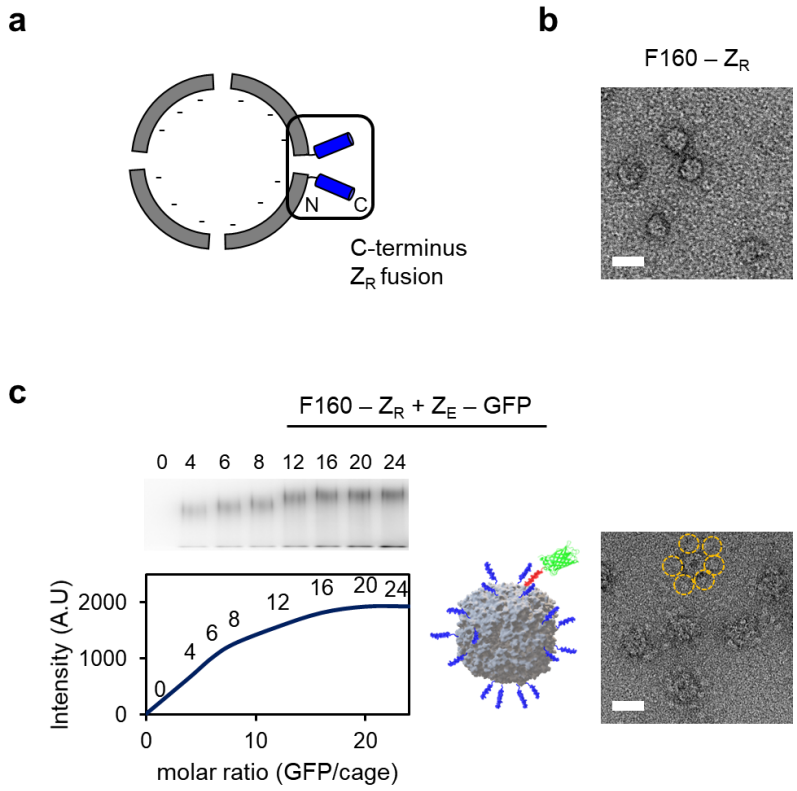

Figure S7. Construction of fully exposed Z_R ferritins (F160-Z_R). (a) Schematic diagram of zipper exposure on an E-helix truncated F160 surface. Zipper peptides fused to the F160 C-termini are fully exposed. (b) TEM image of F160-Z_R. (c) Gel shift assay of F160-Z_R binding to Z_E-GFPs with increased GFP per cage ratios (0 to 24). A TEM image and the schematic structure of F160-Z_R bound with Z_E-GFP. Scale bars 20 nm.

Note: The mixture of F160-Z_R and Z_E-GFP was applied for SEC to remove unbound GFPs before TEM analysis.

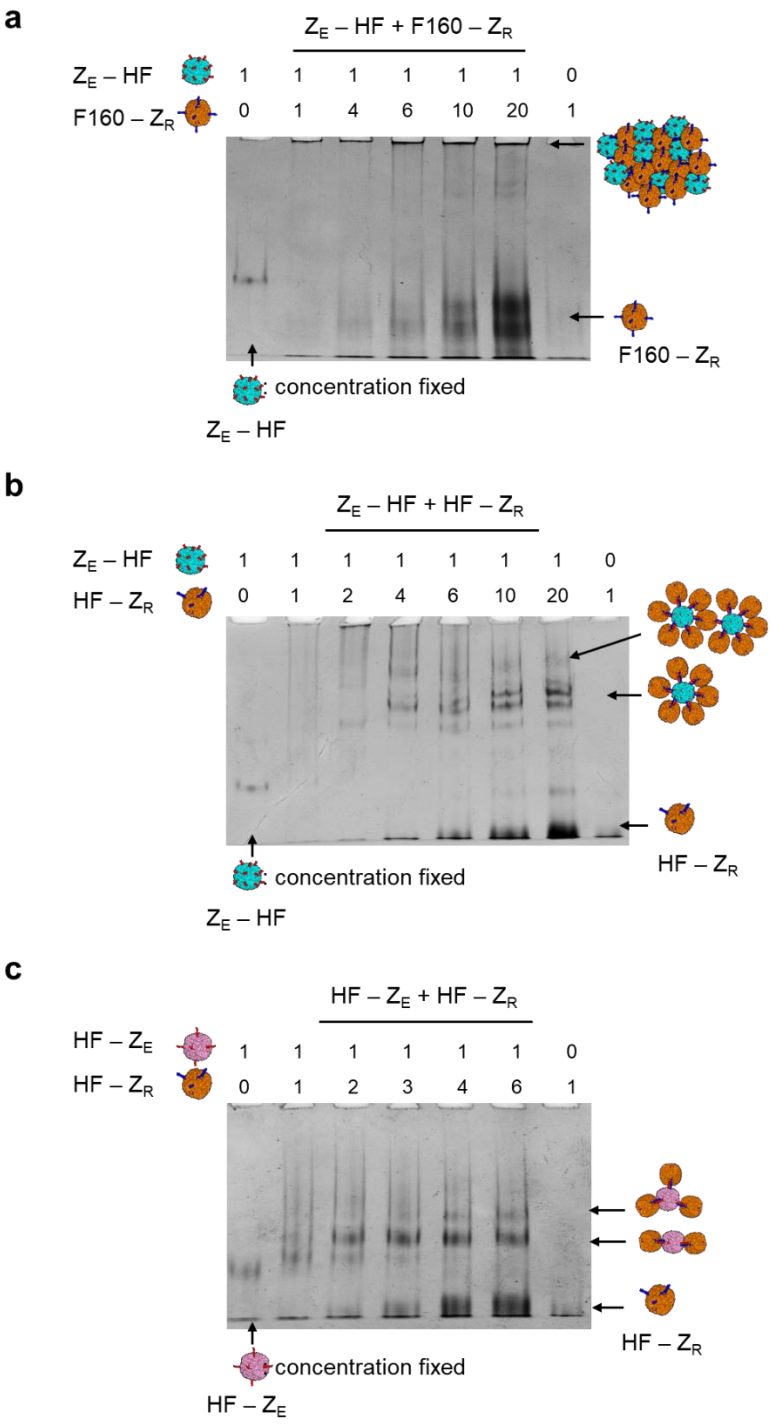

Figure S8. Native gel shift assays of fully exposed F160-Z_R and anisotropic HF-Z_R binding to fully exposed Z_E-HF and HF-Z_E at varying ratios. (a) Z_E-HF + F160-Z_R. (b) Z_E -HF + HF-Z_R. (c) HF-Z_E + HF-Z_R. Probable cage-to-cage assemblies are indicated with arrows and schematic diagrams.

Note: Schematic structural diagrams with the number of bound HF-Z_R were examined and discussed in Figure S15. Large cage aggragates of the Z_E-HF + F160-Z_R mixture stay at the top of gels (Figure S8a).

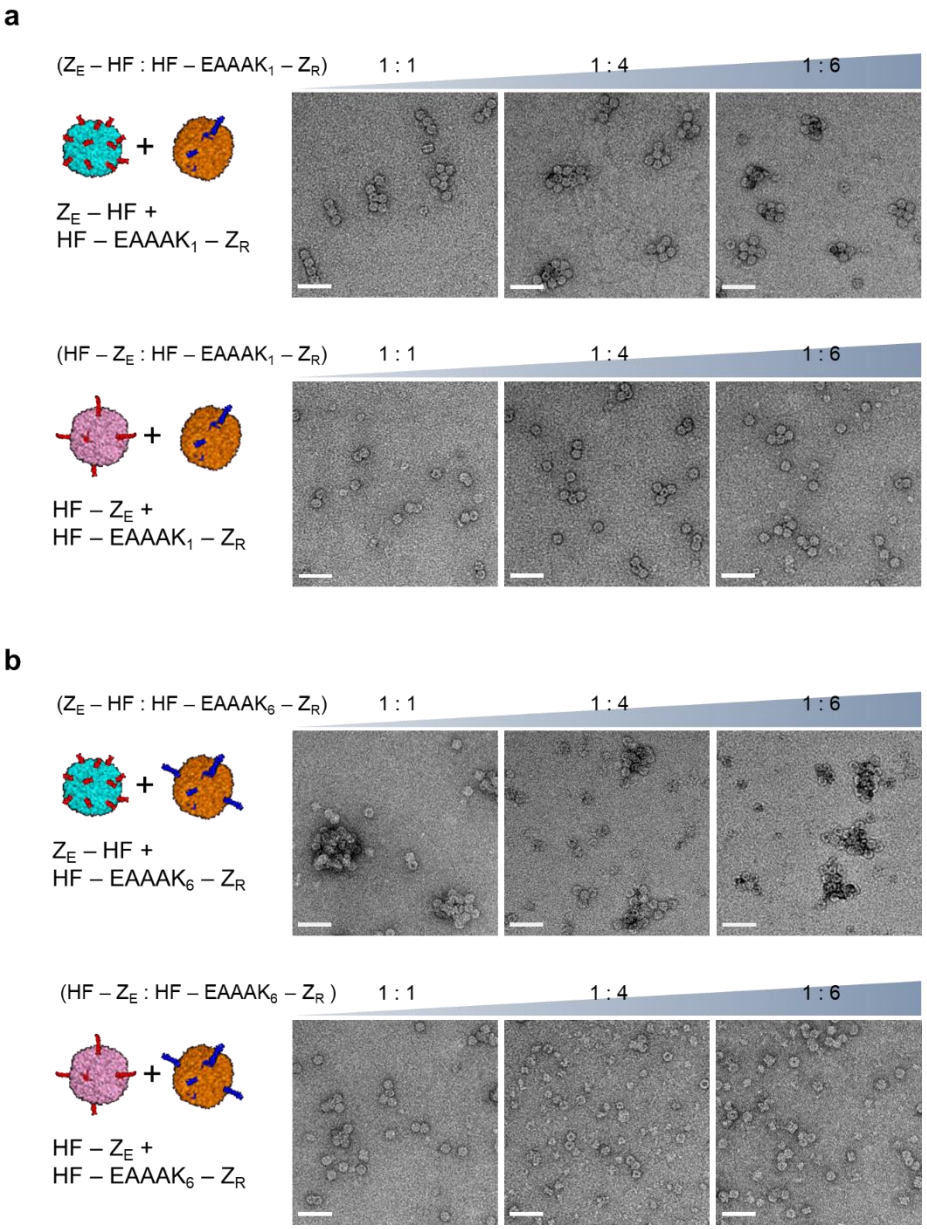

Figure S9. High order cage assembly of anisotropic HF-Z_R with different linker lengths. (a) TEM images of Z_E ferritin (Z_E-HF, HF-Z_E) and (the shorter linker variant) HF-EAAAK$_1$-Z_R mixtures with increased HF-EAAAK$_1$-Z_R. (Z_E ferritin: HF-EAAAK$_1$-Z_R = 1:1, 1:4, and 1:6) (b) TEM images of Z_E ferritin (Z_E-HF, HF-Z_E) and (the longer linker variant) HF-EAAAK$_6$-Z_R mixtures with increased HF-EAAAK$_6$-Z_R. (Z_E ferritin: HF-EAAAK$_6$-Z_R = 1:1, 1:4, and 1:6) Scale bars 50 nm.

Note: The shorter linker variant (HF-EAAAK$_1$-Z_R) with fewer surface Z_R was highly effective for constrained assembly, even more than the initial HF-EAAAK$_3$-Z_R. At the Z_E-HF:HF-EAAAK$_1$-Z_R ratio 1:1, continuous cage-to-cage assembly was not observed, while the 1:1 Z_E-HF/HF-EAAAK$_3$-Z_R mixture produced fairly large cage assemblages (Figure S9a vs Figure 2b).

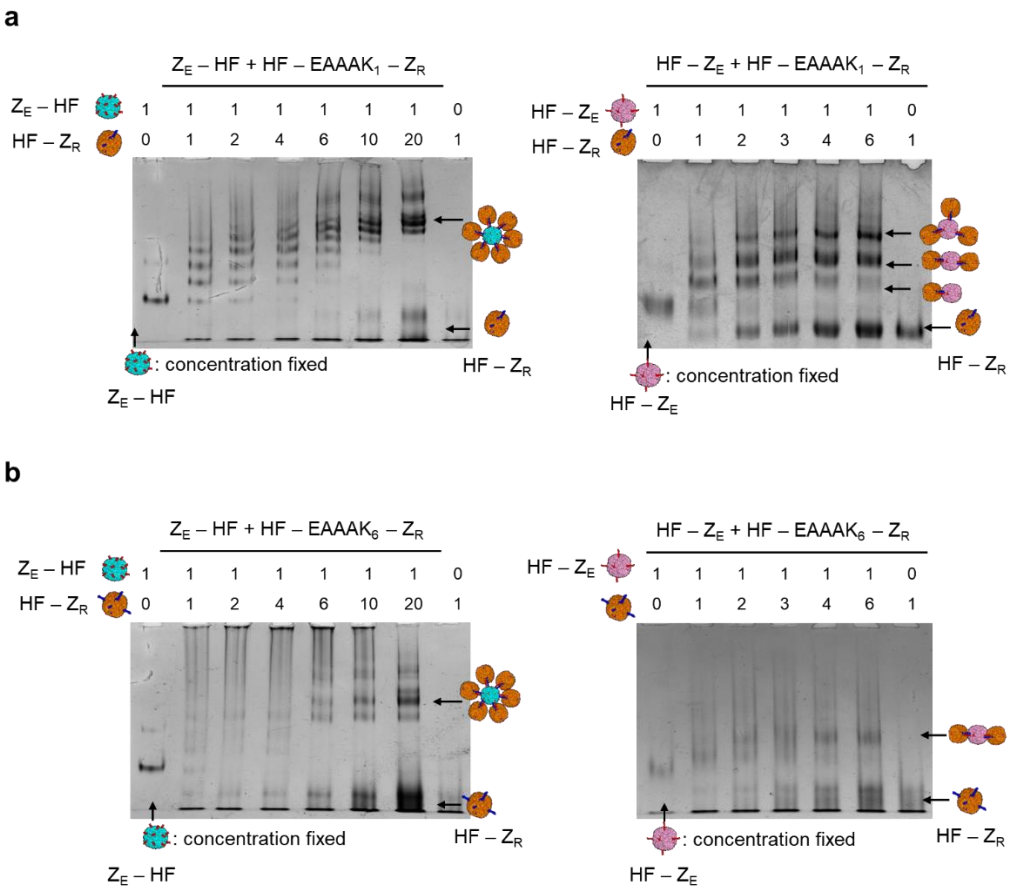

Figure S10. Native gel shift assays of anisotropic HF-Z_R with different linker lengths binding to fully exposed Z_E-HF and HF-Z_E at varying ratios. (a) HF-EAAAK$_1$-Z_R. (b) HF-EAAAK$_6$-Z_R.

Note: At the similar Z_E-HF/HF-Z_R ratios, HF-EAAAK$_3$-Z_R binding saturated earlier than HF-EAAAK$_1$-Z_R (Figure S8b vs Figure S10a). It is possible that cage assembly strength was slightly weaker for HF-EAAAK$_1$-Z_R than HF-EAAAK$_3$-Z_R, likely due to that multiple Z_E/Z_R interactions can be involved in a single cage-to-cage assembly event for HF-EAAAK$_3$-Z_R but not with HF-EAAAK$_1$-Z_R with fewer surface Z_R.

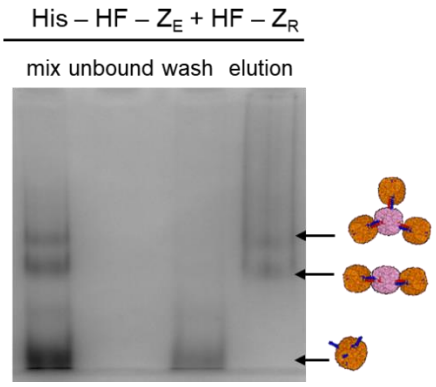

Figure S11. High order ferritin (HF-Z_E:HF-Z_R = 1:6) purification with His affinity chromatography. A native fluorescence gel image of cage mixture (mix), resin-unbound flow through (unbound), washed un-assembled HF-Z_R, and eluted high order structure is shown.

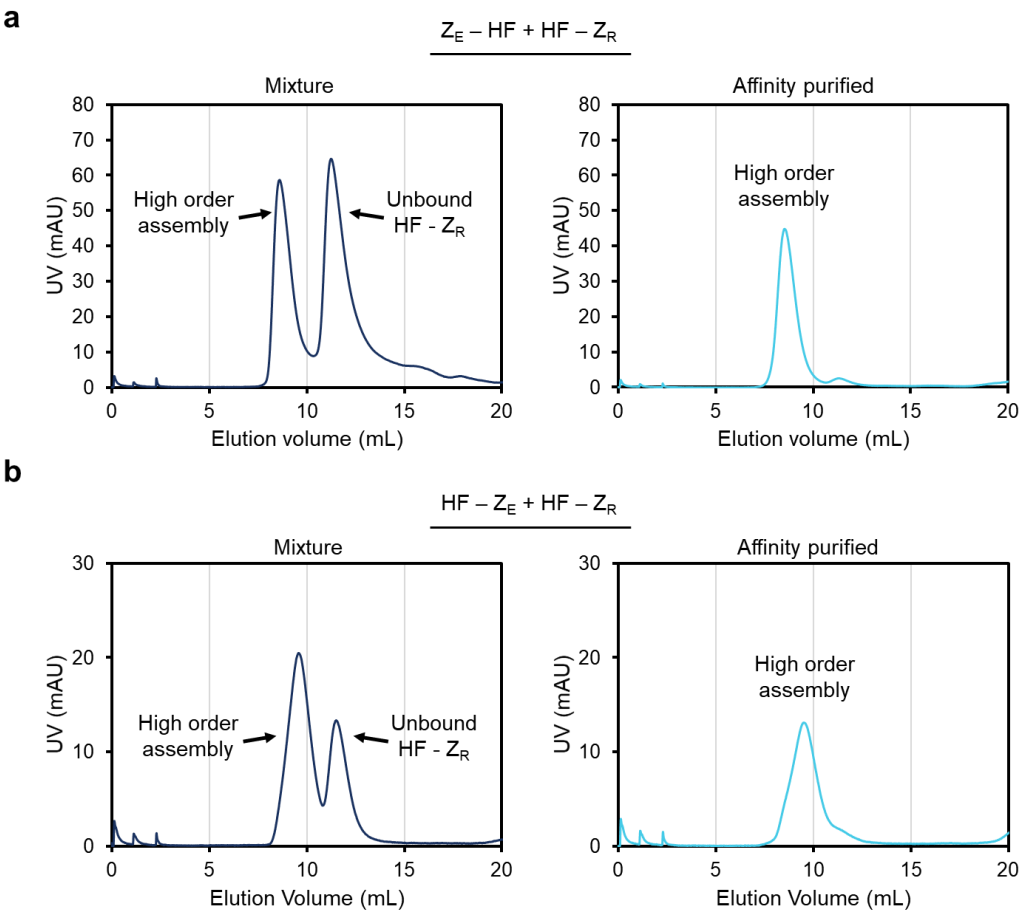

Figure S12. SEC profiles of high order ferritin assemblies before (left) and after (right) His affinity purification. (a) Z_E-HF + HF-Z_R. (b) HF-Z_E + HF-Z_R. Elution peaks for high order assemblies and unbound HF-Z_R are indicated.

Note: Very low levels (< 5%) of unbound HF-Z_R peaks are observed for purified samples, which might be originated in part from dissociation of relatively weakly bound HF-Z_R during SEC.

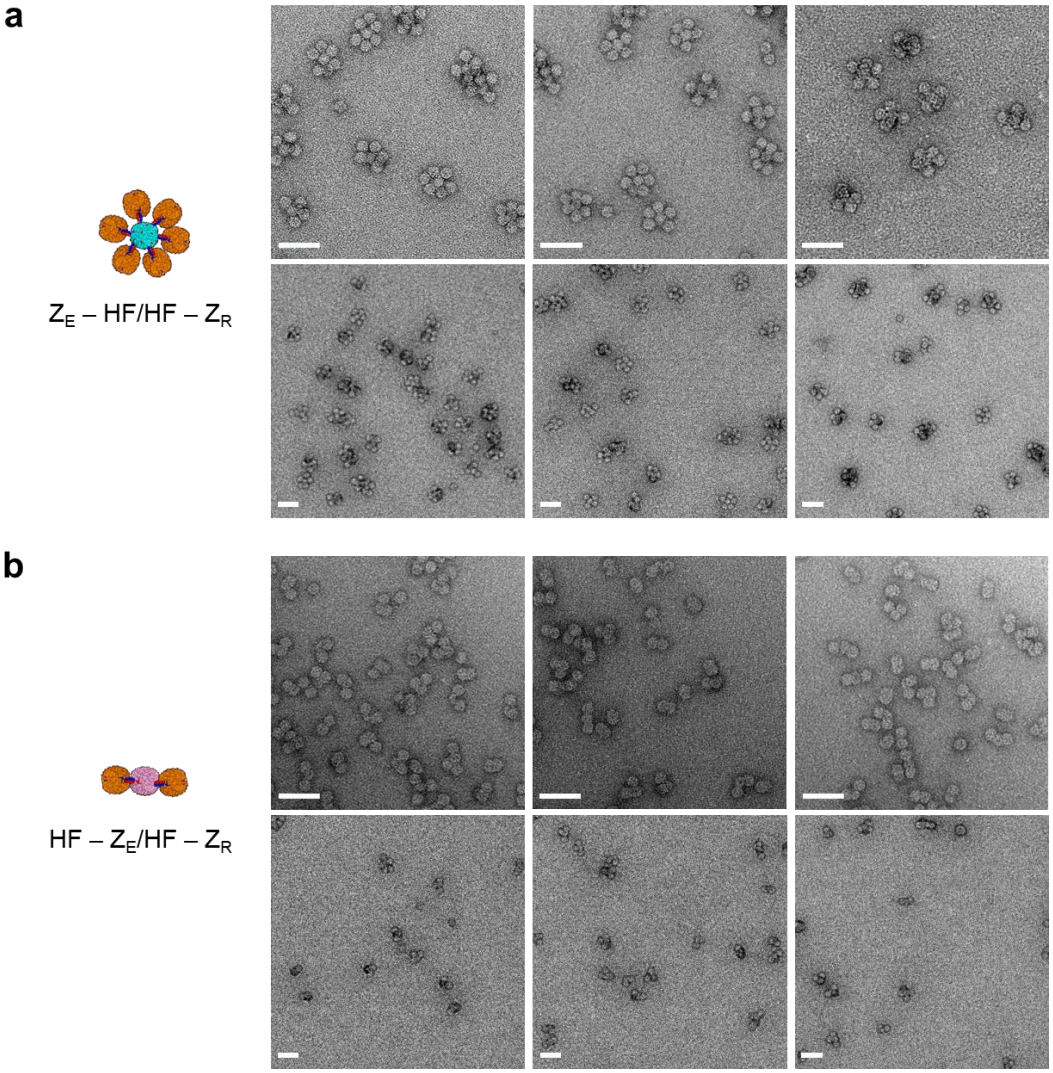

Figure S13. Additional TEM images of affinity purified high order (a) Z_E-HF/HF-Z_R and (b) HF-Z_E/HF-Z_R. Scale bars 50 nm.

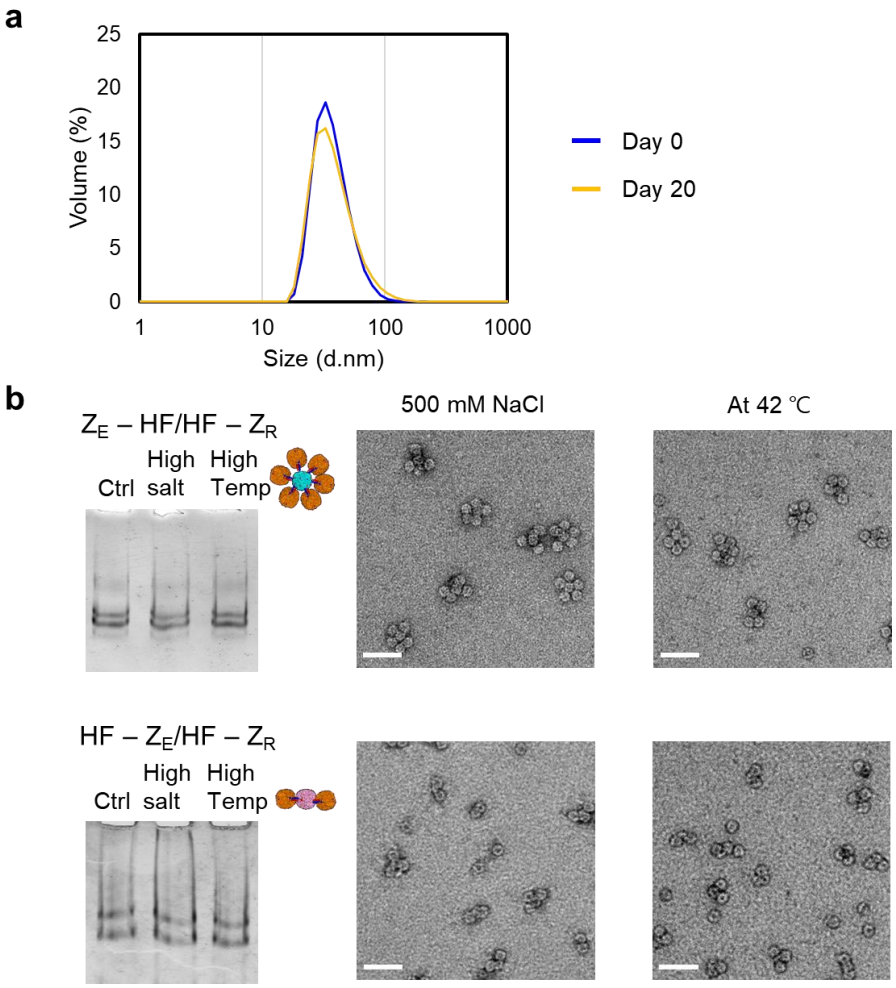

Figure S14. Stability of high order ferritin assemblies. (a) DLS data of high order Z_E-HF/HF-Z_R assemblies before (blue) and after (yellow) 20 days incubation at 4 °C. (b) Native gel and TEM images of purified Z_E-HF/HF-Z_R (top) and HF-Z_E/HF-Z_R (bottom) assemblies after 30 min incubation with 500 mM NaCl or at 42 °C. Scale bars 50 nm.

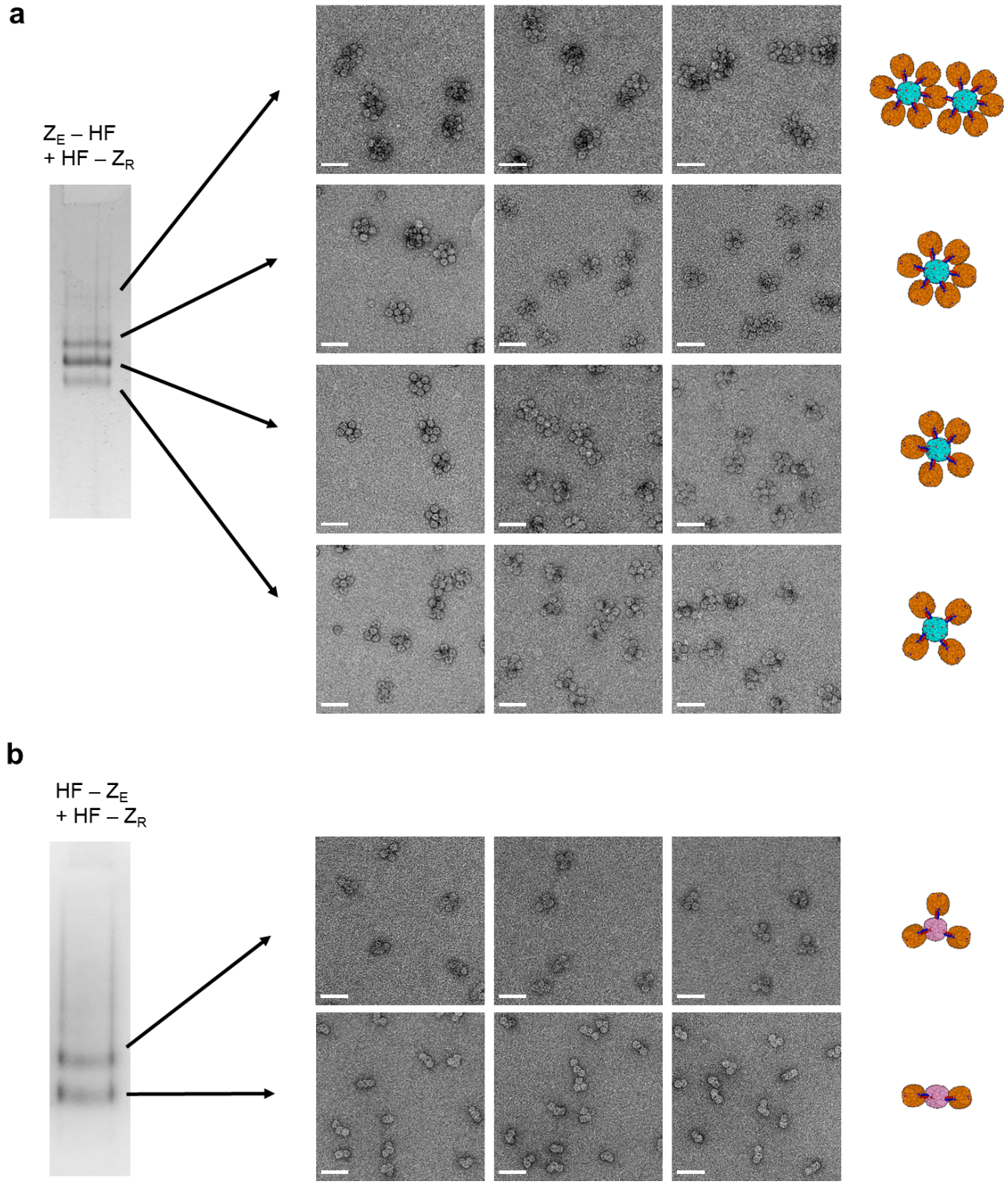

Figure S15. Native gel band analysis. Affinity purified high order ferritin (a) Z_E-HF/HF-Z_R and (b) HF-Z_E/HF-Z_R assemblies were separated in a 3% native gel. Protein assemblies from each gel band were extracted by electro-elution and analyzed by TEM. Scale bars 50 nm.

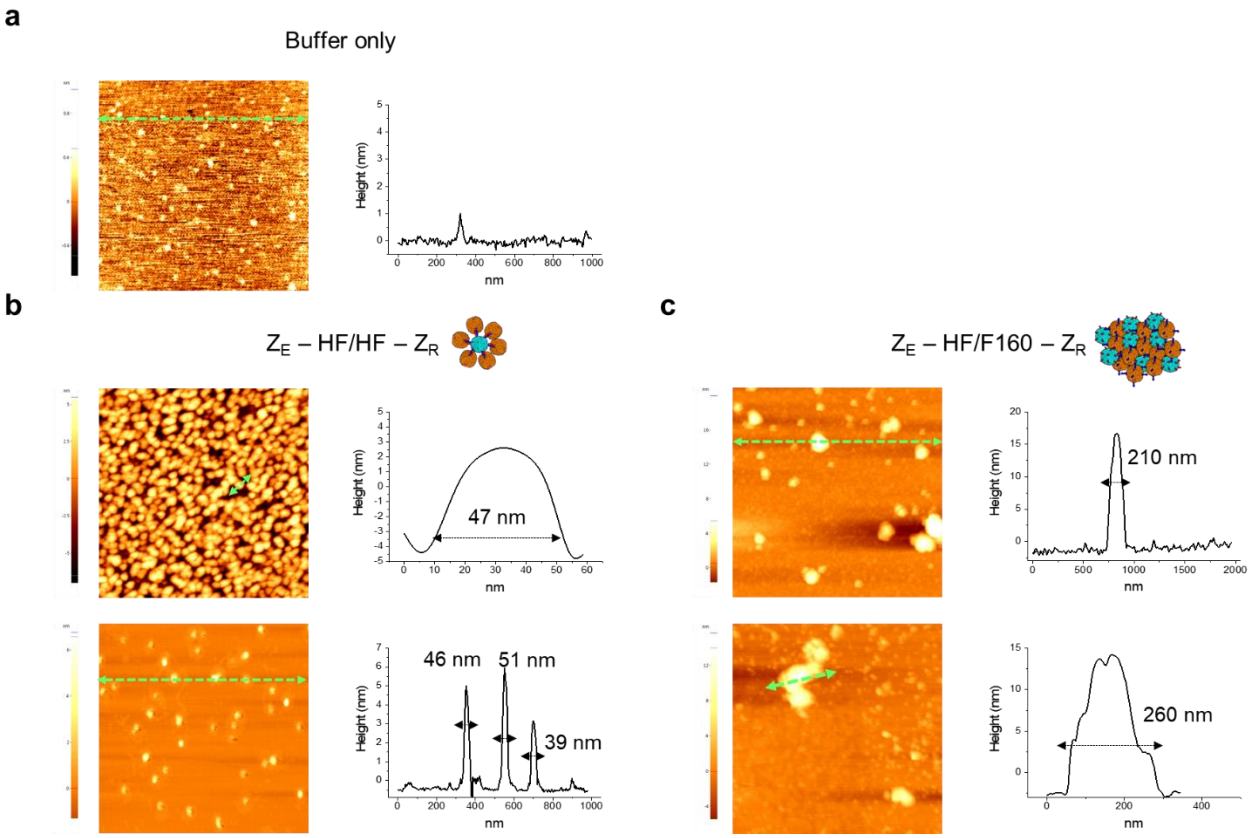

Figure S16. Atomic force microscopy (AFM) micrographs and line profiles of high order ferritins. (a) Mica adsorbed with buffer alone without proteins. (b) Purified high order Z_E-HF/HF-Z_R. Two protein concentrations (0.1 mg/mL (top) and 0.02 mg/mL (bottom)) were examined. (c) Z_E-HF + F160-Z_R mixture. Line profiles were measured along the green arrows in each image.

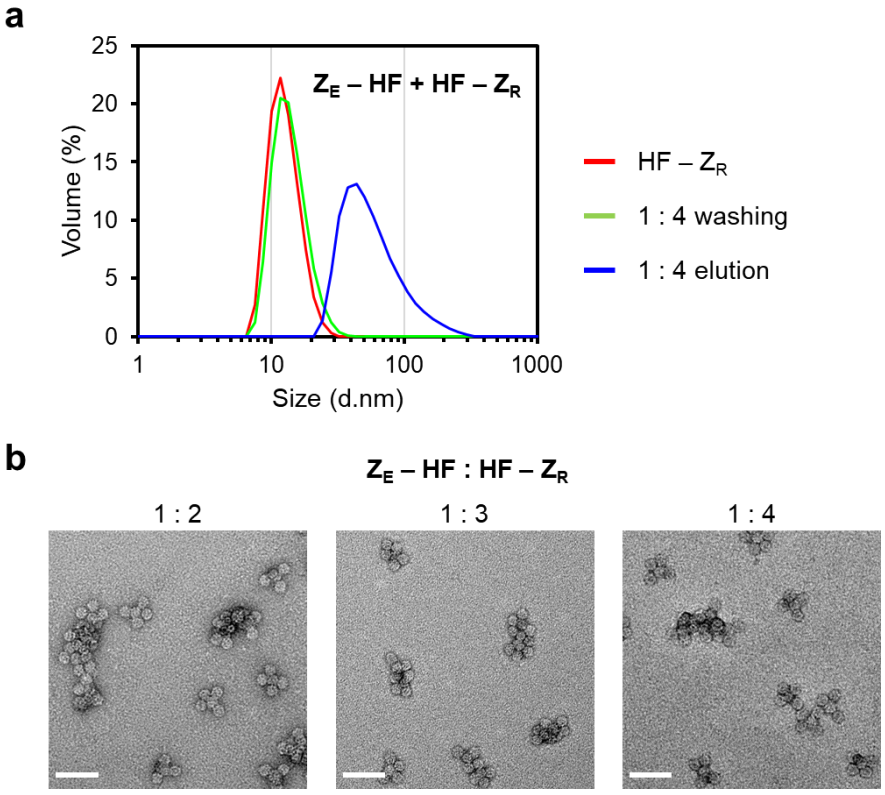

Figure S17. High order Z_E-HF/HF-Z_R assemblies with varying HF-Z_R ratios. (a) DLS data of HF-Z_R (red), un-assembled HF-Z_R (green), and eluted high order structure (blue) for a 1:4 Z_E-HF:HF-Z_R ratio. (b) TEM images of purified high order Z_E-HF/HF-Z_R with varying HF-Z_R ratios. Scale bars 50 nm.

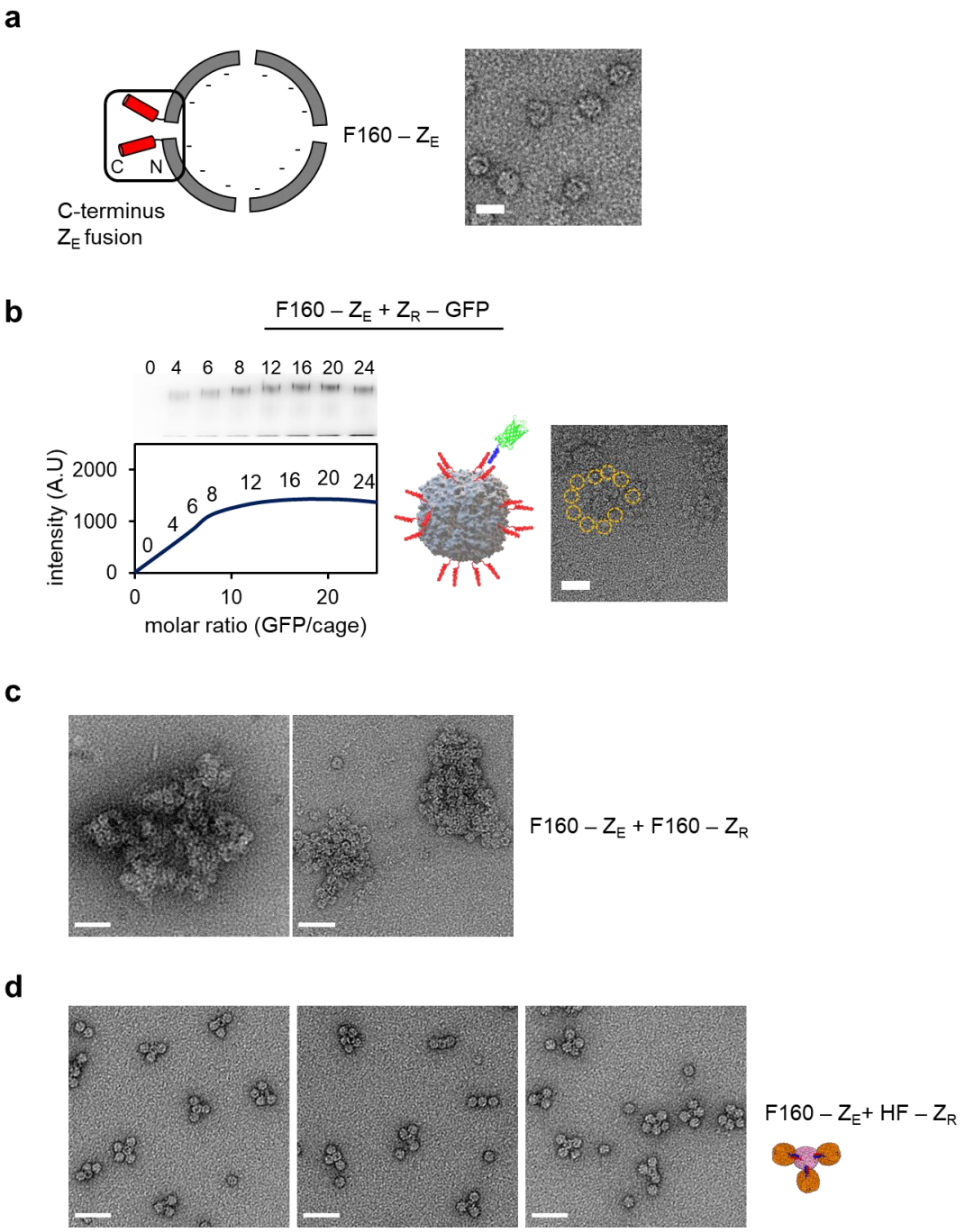

Figure S18. F160-Z_E + HF-Z_R assembly (a) Schematic diagram and TEM image of Z_E exposure on an E-helix truncated F160 surface (F160-Z_E). (b) Gel shift assay of F160-Z_E binding to Z_R-GFPs with increased GFP per cage ratios (0 to 24). A TEM image and the schematic structure of F160-Z_R bound with Z_E-GFP. Scale bars 20 nm. (c) TEM images of the F160-Z_E and F160-Z_R mixtures (1:1 ratio). (d) TEM images of purified high order F160-Z_E+HF-Z_R. Scale bars 50 nm.

Note: The mixture of F160-Z_E and Z_R-GFP was applied for SEC to remove unbound GFPs before TEM analysis (Figure S18b).

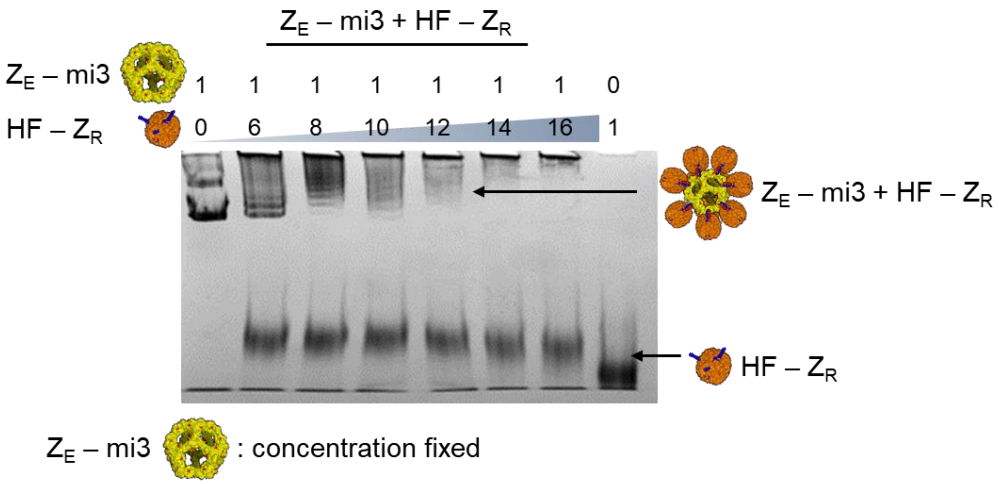

Figure S19. Native gel shift assay of anisotropic HF-Z_R binding to large Z_E-mi3 at varying cage ratios. Probable cages and cage-to-cage assemblies are indicated with arrows and schematic diagrams. The number of bound HF-Z_R can be estimated based on band ladders for cage-to-cage assemblies.

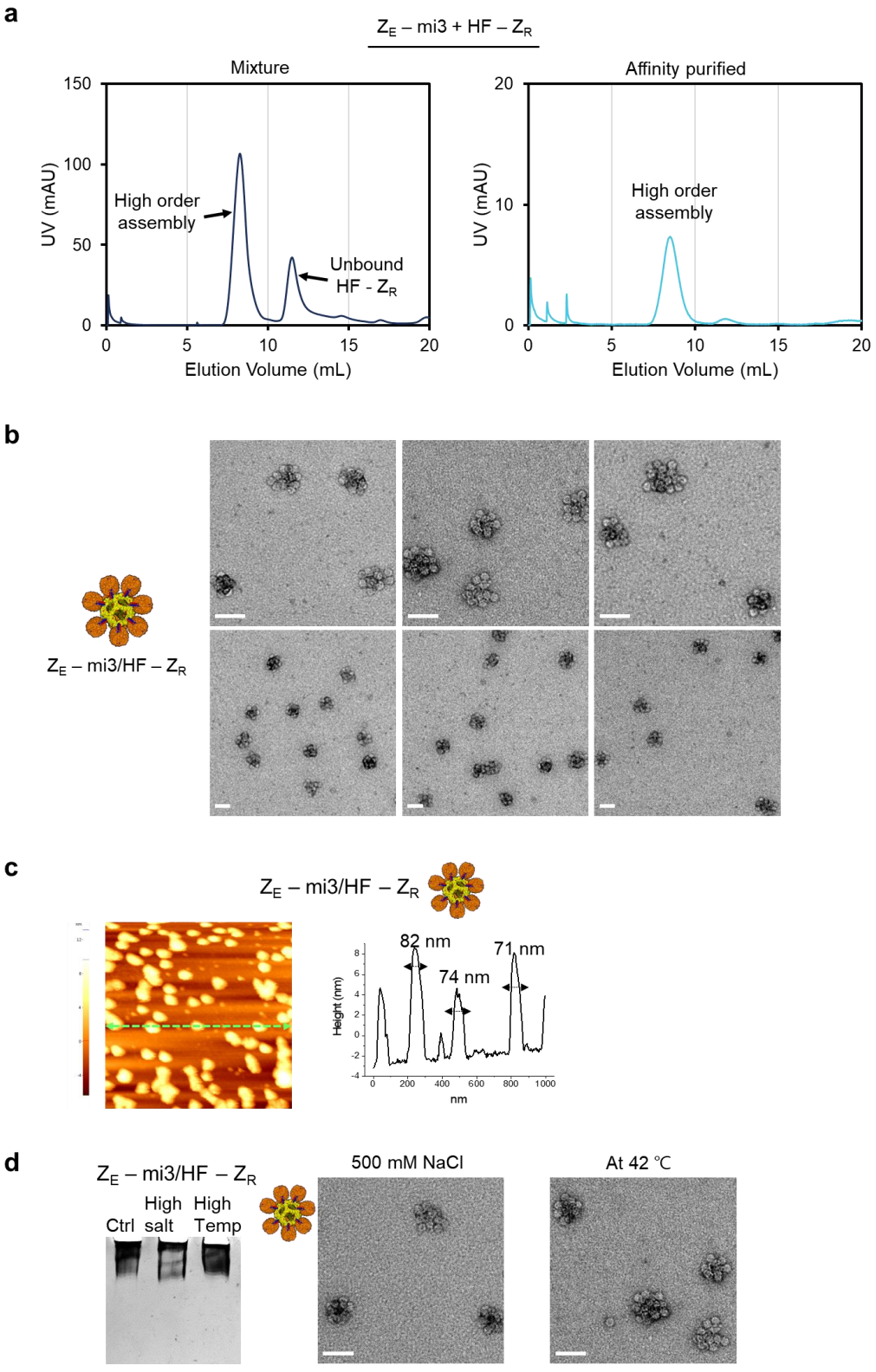

Figure S20. Charcterization of Z_E-mi3/HF-Z_R assemblies. (a) SEC profiles before (left) and after (right) His affinity purification. (b) Addtional TEM images. (c) AFM image and line profile. (d) Stability test against high salt and temperature.

Assemblies	Protein recovery yield (%)
Z_E-HF/HF-Z_R	52
HF-Z_E/HF-Z_R,	56
Z_E-mi3/HF-Z_R	36

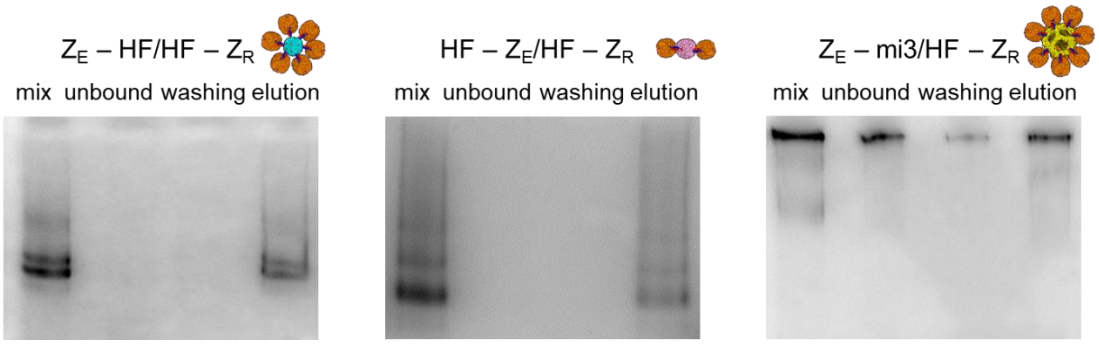

Figure S21. Core cage protein recovery yields. Core cages (Z_E-HF, HF-Z_E, Z_E-mi3) were labeled with Cy5 and mixed with HF-Z_R. After affinity purification, core cage Cy5 intensities of isolated final high order assemblies were compared to the initially added core cage signals.

Protein sequences

(6His tag –) Z_E – HF

M (HHHHHH GGS) KGS LEIEAAALEQ ENTALETEVA ELEQEVQRLE NIVSQYRTRY GPL GGG SGG GTG GGS GGG EFTTASTSQVR QNYHQDSEAA INRQINLELYASYVYLSMSY YFDRDDVALK NFAKYFLHQSHEEREHAEKL MKLQNQRGGR IFLQDIKKPD CDDWESGLNA MECALHLEKN VNQSLLELHK LATDKNDPHL CDFIETHYLN EQVKAIKELG DHVTNLRKMG APESGLAEYL FDKHTLGDSD NES

orange: 6His tag, red: Z_E, violet: flexible linker, black: ferritin

(6His tag –) HF – Z_E

M (HHHHHH GGS) TTASTSQVR QNYHQDSEAA INRQINLELY ASYVYLSMSY YFDRDDVALK NFAKYFLHQS HEEREHAEKL MKLQNQRGGR IFLQDIKKPD CDDWESGLNA MECALHLEKN VNQSLLELHK LATDKNDPHL CDFIETHYLN EQVKAIKELG DHVTNLRKMG APESGLAEYL FDKHTLGDSD NES GGG SGG GTG GGS GGG EF LEIEAAALEQ ENTALETEVA ELEQEVQRLE NIVSQYRTRY GPL

HF – Z_R

MTTASTSQVR QNYHQDSEAA INRQINLELY ASYVYLSMSY YFDRDDVALK NFAKYFLHQS HEEREHAEKL MKLQNQRGGR IFLQDIKKPD CDDWESGLNA MECALHLEKN VNQSLLELHK LATDKNDPHL CDFIETHYLN EQVKAIKELG DHVTNLRKMG APESGLAEYL FDKHTLGDSD NES GS EAAAK EAAAK EAAAK EF GS NTALRTRVA ELRQRVQRLR NEVSQYETRY GPL

yellow: rigid linker, blue: Z_R

HF – Z_R Linker variants: linker-less

MTTASTSQVR QNYHQDSEAA INRQINLELY ASYVYLSMSY YFDRDDVALK NFAKYFLHQS HEEREHAEKL MKLQNQRGGR IFLQDIKKPD CDDWESGLNA MECALHLEKN VNQSLLELHK LATDKNDPHL CDFIETHYLN EQVKAIKELG DHVTNLRKMG APESGLAEYL FDKHTLGDSD NES EF GS NTALRTRVA ELRQRVQRLR NEVSQYETRY GPL

HF – Z_R Linker variants: flexible linker (GGS_5)

MTTASTSQVR QNYHQDSEAA INRQINLELY ASYVYLSMSY YFDRDDVALK NFAKYFLHQS HEEREHAEKL MKLQNQRGGR IFLQDIKKPD CDDWESGLNA MECALHLEKN VNQSLLELHK LATDKNDPHL CDFIETHYLN EQVKAIKELG DHVTNLRKMG APESGLAEYL FDKHTLGDSD NES GGG SGG GTG GGS GGG EF GS NTALRTRVA ELRQRVQRLR NEVSQYETRY GPL

HF – Z_R Linker variants: short linker ($EAAAK_1$)

MTTASTSQVR QNYHQDSEAA INRQINLELY ASYVYLSMSY YFDRDDVALK NFAKYFLHQS HEEREHAEKL MKLQNQRGGR IFLQDIKKPD CDDWESGLNA MECALHLEKN

VNQSLLELHK LATDKNDPHL CDFIETHYLN EQVKAIKELG DHVTNLRKMG APESGLAEYL FDKHTLGDSD NES GS EAAAK EF GS NTALRTRVA ELRQRVQRLR NEVSQYETRY GPL

HF – Z_R Linker variants: long linker ($EAAAK_6$)

MTTASTSQVR QNYHQDSEAA INRQINLELY ASYVYLSMSY YFDRDDVALK NFAKYFLHQS HEEREHAEKL MKLQNQRGGR IFLQDIKKPD CDDWESGLNA MECALHLEKN VNQSLLELHK LATDKNDPHL CDFIETHYLN EQVKAIKELG DHVTNLRKMG APESGLAEYL FDKHTLGDSD NES GS EAAAK EAAAK EAAAK EAAAK EAAAK EAAAK EF GS NTALRTRVA ELRQRVQRLR NEVSQYETRY GPL

F160 – Z_E

MTTASTSQVR QNYHQDSEAA INRQINLELY ASYVYLSMSY YFDRDDVALK NFAKYFLHQS HEEREHAEKL MKLQNQRGGR IFLQDIKKPD CDDWESGLNA MECALHLEKN VNQSLLELHK LATDKNDPHL CDFIETHYLN EQVKAIKELG DHVTNLRKMG GGG SGG GTG GGS GGG EF LEIEAAALEQ ENTALETEVA ELEQEVQRLE NIVSQYRTRY GPL

black: F160

F160 – Z_R

MTTASTSQVR QNYHQDSEAA INRQINLELY ASYVYLSMSY YFDRDDVALK NFAKYFLHQS HEEREHAEKL MKLQNQRGGR IFLQDIKKPD CDDWESGLNA MECALHLEKN VNQSLLELHK LATDKNDPHL CDFIETHYLN EQVKAIKELG DHVTNLRKMG GGG SGG GTG GGS GGG EF GS NTALRTRVA ELRQRVQRLR NEVSQYETRY GPL

Z_E-GFP

MKGS LEIEAAALEQ ENTALETEVA ELEQEVQRLE NIVSQYRTRY GPL GGG SGG GTG GGS GGG EF GSKGEELFTG VVPILVELDG DVNGHEFSVR GEGEGDATIG ELTLKFICTT GELPVPWPTL VTTLTYGVQC FSRYPDHMKR HDFFKSAMPE GYVQERTISF KDDGKYKTRA VVKFEGDTLV NRIELKGTDF KEDGNILGHK LEYNFNSHDV YITADKQENG IKAEFTVRHN VEDGSVQLAD HYQQNTPIGD GPVLLPDDHY LSTETVLSKD PNEKRDHMVL HEYVNAAGIT LE HHHHHH

green: GFP

Z_R-GFP

MKGS NTALRTRVA ELRQRVQRLR NEVSQYETRY GPL GGG SGG GTG GGS GGG GS

GSKGEELFTG VVPILVELDG DVNGHEFSVR GEGEGDATIG ELTLKFICTT GELPVPWPTL VTTLTYGVQC FSRYPDHMKR HDFFKSAMPE GYVQERTISF KDDGKYKTRA VVKFEGDTLV NRIELKGTDF KEDGNILGHK LEYNFNSHDV YITADKQENG IKAEFTVRHN VEDGSVQLAD HYQQNTPIGD GPVLLPDDHY LSTETVLSKD PNEKRDHMVL HEYVNAAGIT LE HHHHHH

GFP-HF

GSKGEELFTG VVPILVELDG DVNGHEFSVR GEGEGDATIG ELTLKFICTT GELPVPWPTL VTTLTYGVQC FSRYPDHMKR HDFFKSAMPE GYVQERTISF KDDGKYKTRA VVKFEGDTLV NRIELKGTDF KEDGNILGHK LEYNFNSHDV YITADKQENG IKAEFTVRHN VEDGSVQLAD HYQQNTPIGD GPVLLPDDHY LSTETVLSKD PNEKRDHMVL HEYVNAAGIT LE GGG SGG GTG GGS GGG EF MTTASTSQVR QNYHQDSEAA INRQINLELY ASYVYLSMSY YFDRDDVALK NFAKYFLHQS HEEREHAEKL MKLQNQRGGR IFLQDIKKPD CDDWESGLNA MECALHLEKN VNQSLLELHK LATDKNDPHL CDFIETHYLN EQVKAIKELG DHVTNLRKMG APESGLAEYL FDKHTLGDSD NES

6His tag–Z_E-mi3

MHHHHHH GGS LEIEAAALEQ ENTALETEVA ELEQEVQRLE NIVSQYRTRY GPL GGG SGG GTG GGS GGG EF KMEELFKKHK IVAVLRANSV EEAKKKALAV FLGGVHLIEI TFTVPDADTV IKELSFLKEM GAIIGAGTVT SVEQARKAVE SGAEFIVSPH LDEEISQFAK EKGVFYMPGV MTPTELVKAM KLGHTILKLF PGEVVGPQFVK AMKGPFPNVKFV PTGGVNLDNVC EWFKAGVLAVG VGSALVKGTP VEVAEKAKAF VEKIRGCTE

sky blue: mi3

(6His tag – Z_E–) Ferritin di-subunit

M (HHHHHH GGS) LEIEAAALEQ ENTALETEVA ELEQEVQRLE NIVSQYRTRY GPL TTASTSQVR QNYHQDSEAA INRQINLELY ASYVYLSMSY YFDRDDVALK NFAKYFLHQS HEEREHAEKL MKLQNQRGGR IFLQDIKKPD CDDWESGLNA MECALHLEKN VNQSLLELHK LATDKNDPHL CDFIETHYLN EQVKAIKELG DHVTNLRKMG APESGLAEYL FDKHTLGDSD NES GGS GVS GGT GGS GGR GSGPLGVRGKEF GGS GGS GGT GGS GGS MTTASTSQVR QNYHQDSEAA INRQINLELY ASYVYLSMSY YFDRDDVALK NFAKYFLHQS HEEREHAEKL MKLQNQRGGR IFLQDIKKPD CDDWESGLNA MECALHLEKN VNQSLLELHK LATDKNDPHL CDFIETHYLN EQVKAIKELG DHVTNLRKMG APESGLAEYL FDKHTLGDSD NES

Experimental Methods

Preparation of engineered ferritins. Genes for the human H-chain ferritin, F160, zipper ferritin variants, zipper-GFP variants, mi3, and di-monomer subunit were cloned into the pET-21a(+) plasmid (Novagen). Cloned plasmids were transformed into BL21(DE3), and the cells were grown in LB until the A600 reaches 0.6. 1 mM IPTG (LPS solution) was added, and the cells were incubated overnight at 20 °C. Protein expressing cells were harvested by centrifugation and sonicated. The cell lysates were centrifuged at 12000 rpm for 15 min. Supernatants of products were heated at 60 °C for 10 min, and aggregates were removed by centrifugation at 12000 rpm for 15 min. Finally, proteins were purified by FPLC (Fast Protein Liquid Chromatography) with a Sepacryl S-300 column (buffer: Tris 50 mM, NaCl 150 mM, pH 7.2). For His modified cage protein variants, pellets of centrifuged cell lysates were resuspended and sonicated with mild condition (resuspension buffer: Tris 50 mM, NaCl 150 mM, EDTA 2 mM, pH 7.2). Again, products were heated at 60 °C for 10 min and centrifuged at 12000 rpm for 15 min, followed by FPLC purification.

Negative-stained Transmission Electron Microscopy (TEM). For negative-stain TEM analyses, samples (0.03 mg/mL) were adsorbed onto a glow-discharged carbon-coated grid (200 mesh) for 2 min. The grid was washed with distilled water twice. To achieve negative staining, 2% uranyl acetate was treated for 1 min, and the grid was dried by air for 10 min. Samples were investigated by Tecnai G2 F30 S-Twin 300 kv TEM. Images were taken at a magnification of ×25,000, ×49,000 or ×75,000 depending on the size of proteins.

High order ferritin construction. 6His- and Z_E-fused core ferritins (0.05 μM) were mixed with the Z_R-fused anisotropic ferritins at the indicated concentration ratios. After reacting for 3 h, mixtures were incubated with pre-equilibrated Ni-IDA resin (equilibrium buffer: Tris 50 mM, NaCl 500 mM, imidazole 10 mM) for 30 min (20 °C, in a shaker incubator). The resin containing samples were transferred to an empty column, and unbound HF-Z_R cages were washed (washing buffer: Tris 50 mM, NaCl 500 mM, imidazole 100 mM), followed by high order ferritin elution (elution buffer: Tris 50 mM, NaCl 150 mM, imidazole 500 mM). 50 μM EDTA were added to the purified protein solution to remove free nickel ions, and the solution was dialyzed twice in 1× PBS. Isolated assemblies could be stored at 4 °C for over a month without any aggregation or disassembly. For protein recovery yield calculation, core cage proteins were tagged with NHS-Cyanine 5 (Cy5). Protein recovery yields after assembly formation and His affinity purification were calculated by comparing fluorescence intensities before and after purification (Varioskan Flash, Thermofisher). SEC elution profiles of high order ferritin assemblies before after His purification were obtained with a Superdex 200 column (buffer: 1× PBS).

Electrophoretic mobility shift assay. Protein mixtures or affinity purified assemblies were applied to 3% native PAGE gels. Shifted bands (GFP or Cy5 fluorescence) were imaged by ChemiDoc MP (Biorad). Quantitative data were obtained by the Image Lab TM 6.0.1(Biorad) software. For GFP binding titration, zipper ferritin variants (0.4 μM) were mixed with their complementary zipper-fused

GFPs with various ratios (buffer: Tris 50 mM, NaCl 150 mM, pH 7.2). After reacting for 6 h, unbound GFPs were removed with a Sepacryl S-300 column (buffer: Tris 50 mM, NaCl 150 mM, pH 7.2), and the resulting proteins were analyzed with a 4% native PAGE gel.

Dynamic Light Scattering (DLS). Protein solutions (0.1 mg/mL, 1 mL) were placed inside disposable polystyrene cuvettes (Sarstedt) and subjected to a Zetasizer Nano ZS DLS instrument (Malvern Instruments). Each sample was averaged following ten measurement runs at room temperature. Data processing was performed using Malvern Zetasizer software.

Atomic Force Microscopy (AFM). Protein samples (0.02 mg/mL, in Tris 50 mM, NaCl 150 mM, 10 % Glycerol) were adsorbed onto a freshly cleaved mica disc (Probes) for 10 min. The mica was washed twice with distilled water, and dried at room temperature. Samples were examined using Park NX10 AFM (Park Systems). Images were collected in tapping mode at a scanning rate of 0.4 Hz. The acquired images have a resolution of 256×256 pixels.

Multimeric ferritin construction. The tandem repeat ferritin subunit was expressed in cells, and the assembled multimeric ferritins were discretely purified by gel separation and subsequent gel electro-elution, as previously described.[1] Briefly, ferritin multimers were separated on a 4% native PAGE gel (HSI SG 600 Series, Hoefer Scientific Instruments, 16 × 18 cm). After electrophoresis, bands for each ferritin multimer were excised. The sliced gels were introduced into a dialysis membrane (Spectrum Labs, MWCO 3,500), and the electrode running buffer (buffer: Tris 25 mM, Glycine 150 mM) was added to the dialysis bag. Ferritin multimers were electro-eluted from the gel at 100 V for 60 min in a horizontal gel electrophoresis apparatus (Mupid-2plus, Takara) at 4 °C with a pre-chilled buffer. Obtained proteins were dialyzed in 1× PBS. High order ferritin assemblies on a 3% native gel were identically isolated by gel electro-elution (Figure S15).

Cellular binding and uptake. HF and HF-Z_R were tagged with NHS-Cyanine 5 (Cy5). HeLa cells were seeded on an 8-well plate (ibidi) (1×10^4 cells per well) and incubated 24 h. For cellular uptake test, 20 nM of ferritins were added to the cells, followed by additional incubation at 37 °C during the indicated time. For cellular binding test, 100 nM of ferritins were added to the cells, followed by additional incubation at 4 °C for 1 h. The treated cells were washed twice with cold Dulbecco's phosphate-buffered saline (DPBS) and fixed with 4% paraformaldehyde solution for 10 min at room temperature. HeLa cells further were stained with 4’,6-diamidino-2-phenylindole (DAPI). Fluorescence images were obtained by using the LSM 800 confocal laser scanning microscope (Carl Zeiss). Quantitative data was obtained by the ZEISS Zen 2.5 software (Carl Zeiss).

1. Y. E. Kim, Y. N. Kim, J. A. Kim, H. M. Kim and Y. Jung, *Nat. Commun.*, 2015, **6**, 7134.